Numerical Uncertainty Analysis for Ship Hydrodynamics Computation

Byung-Soo Kim, Shuguang Wang, Yonghwan Kim
Department of Naval Architecture and Ocean Engineering
Seoul National University, Seoul, Korea
Email: bsbckim@snu.ac.kr

1 INTRODUCTION

Every measured data contains an error compared to the real value. This is due to the inaccuracy of the measurement device, round-off errors, different physical conditions, etc. As the measured data is one of the key sources for analyzing the physical phenomenon, the reliability of the data should be carefully checked. An uncertainty analysis is widely applied to experimental data. The goal of uncertainty analysis is to show the quantitative uncertainty level as a guideline for the people who use the experiment data. Recently, other than the experimental method, numerical simulations are widely applied to analyze physical phenomenon. Similar to physical measurement, numerical computation also contains errors from different sources. A numerical uncertainty analysis is needed in two aspects: 1) to gain evidence/reliability of the numerical solution, and 2) to understand the uncertainty level to be compared with the experimental data. In this study, numerical uncertainty analyses for steady resistance and ship motion problems are carried out, and the abstract introduces some results.

2 METHODOLOGY

2.1 Uncertainty analysis of numerical computation

ITTC recommended guideline [1], followed by Roache [2], divides the numerical uncertainty into two parts depending on the source of the uncertainty. One source of uncertainty is numerical errors, and the analysis of this uncertainty is known as a "verification". The other is modeling errors and their analysis is known as the "validation" step. For the validation, experimental results and their uncertainties are required. In this work, the verification procedure is mostly investigated.

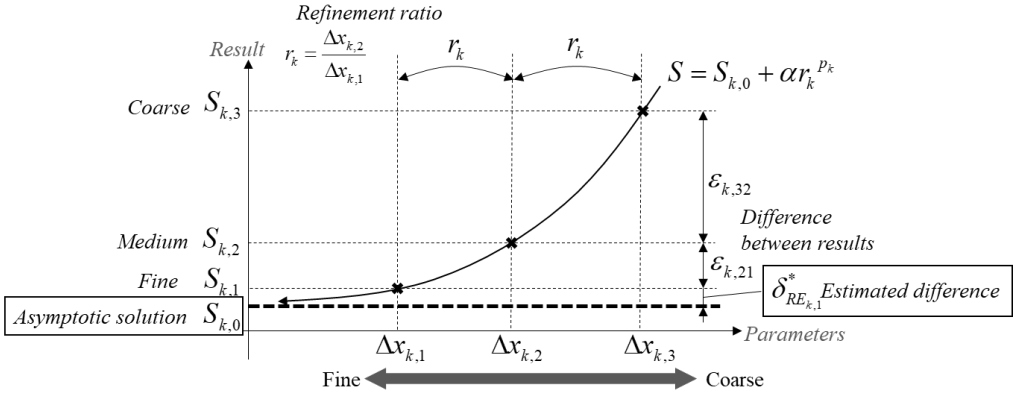

Figure 1: Definition of variables for monotonically convergent computation

The verification analysis requires at least three results(S) using different values of certain discretization parameters(Δx_k), which is also known as sensitivity tests. For the ideal numerical computations, there is a basic assumption that if the discretization parameter is close to zero, the resultant value will converge asymptotically to the final convergent value. However, for the actual numerical computations, different types of convergence criteria can be found. This can be identified using a convergence ratio(R_k), defined as Eq. (1). For the convergent state, the absolute

value of the convergence ratio is smaller than one ($|R_k| < 1$). It has oscillatory behavior if the convergence ratio is smaller than zero ($R_k < 0$), while monotonic behavior will be shown for the bigger value, i.e. $R_k > 0$.

$$R_k = \frac{\varepsilon_{k,32}}{\varepsilon_{k,21}} \tag{1}$$

The final output value of numerical uncertainty(U_k) is similar to expanded uncertainty in experimental uncertainty analysis. This means that the true value of the numerical calculation is inside the interval of $\pm U_k$ with a certain probability level, and 95% probability is a typical expectation. The numerical uncertainty is calculated differently for each case. following ITTC guidelines [1]. First, for the ideal monotonic convergent condition, an asymptotic solution($S_{k,0}$) can be obtained by using Richardson extrapolation (Fig. 1). If the refinement ratio(r_k) is constant, order of accurac (p_k) and the expected numerical difference($\delta^*_{RE,k}$) between the convergent value and the current solution can be obtained using Eq. (2).

$$\delta^*_{RE_{k,1}} = \frac{\varepsilon_{k,21}}{r_k^{\,p_k} - 1} \qquad \text{where,} \quad p_k = \frac{\ln\left|\varepsilon_{k,32} / \varepsilon_{k,21}\right|}{\ln\left(r_k\right)} \tag{2}$$

Based on the computed $\delta^*_{RE,k}$, Roache [2] and Stern et al. [3] proposed factors of safety (FS) method(Eq. 3) and correction factor(CF) method(Eq. 4), respectively.

$$U_{k,\mathrm{FS}} = F_S \left|\delta^*_{RE_{k,1}}\right| \quad \text{where,} \quad F_S = 1.25 \tag{3}$$

$$U_{k,CF} = \begin{cases} \left[9.6\left(1-C_k\right)^2 + 1.1\right]\left|\delta^*_{RE_{k,1}}\right| & \left|1-C_k\right| < 0.125 \\ \left[2\left|1-C_k\right| + 1\right]\left|\delta^*_{RE_{k,1}}\right| & \left|1-C_k\right| \geq 0.125 \end{cases} \tag{4}$$

$$\text{where,} \quad C_k = \frac{r_k^{\,p_k} - 1}{r_k^{\,p_{k,est}} - 1},\ p_{k,est} = \text{theoretical } p_k$$

For the oscillatory conditions(OC), uncertainty is computed based on the maximum and minimum result (Eq. 5). Finally, for the divergent case, uncertainty estimation is not done.

$$U_{k,\mathrm{OC}} = \frac{1}{2}\left(S_{\max} - S_{\min}\right) \tag{5}$$

2.2 Computation method

In this study, the snuMHLFoam which is a customized OpenFOAM-based CFD code is applied for numerical computation and uncertainty analysis. This program adopts the Reynolds-Averaged Navier-Stokes(RANS) equation with continuity equation for two-phase flow. For Reynolds's stress term, the Boussinesq equation is applied with the turbulent viscosity computed by stabilized k-ω SST model. In the stabilized k-ω SST model, an additional buoyancy term and limiter are applied to the original k-ω SST model.

3 COMPUTATION RESULTS

3.1 Calm water resistance

For calm water resistance computation, uncertainty analysis is performed for the total resistance coefficient(C_T), the resistance component from the normal force(C_P), and the resistance component

from the tangential force(C_F). In this case, a varying parameter is a mesh size. The calculation is done for the KCS hull, a popular modern containership model, and different Froude number(Fr) conditions are considered. For the total resistance coefficient, all the cases show monotonic convergence, while dividing it into pressure and viscous components makes the different convergence behaviors for each case. For the finest case, the uncertainty range based on the maximum uncertainty value from the analysis is plotted together in Fig. 2. Although the uncertainty of the total resistance is small for the design speed, for a different ship speed, the uncertainty level varies with the similar mesh resolution. This is in accordance with the fact that physical phenomena differ depending on the ship speed. For the pressure and viscous component coefficient, most cases are oscillatory resulting in relatively smaller uncertainty since oscillatory uncertainty is defined using the maximum and the minimum value.

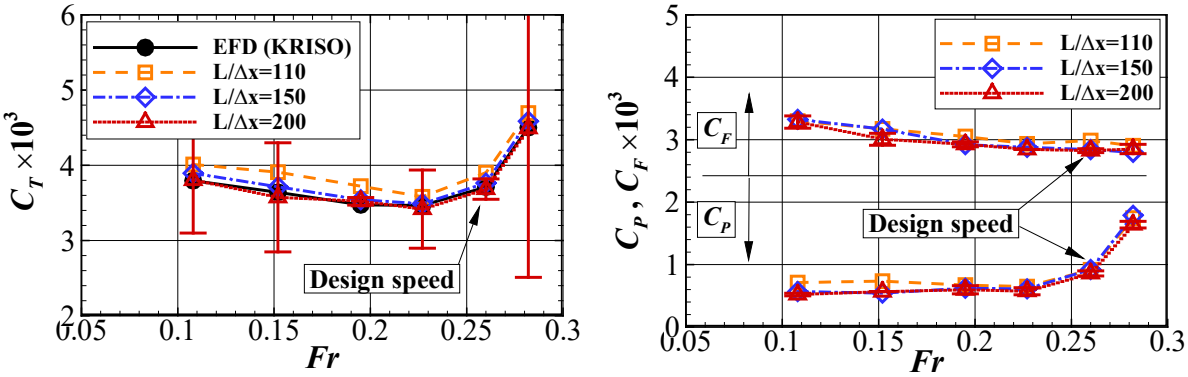

(a) Total resistance coefficient (b) Pressure and frictional coefficient

Figure 2: Uncertainty analysis for KCS hull for different Froude number in calm water

3.2 Motion in head waves

The uncertainty of heave(ξ_3/A) and pitch(ξ_5/kA) motion responses are conducted for a tumblehome [4], [5] in a head sea condition (λ/L = 1.2, H/λ = 1/60, Fr = 0.2). As ship motions are continuously moving, both the mesh size and the time step are varying parameters. When refining the mesh, the aspect ratio is fixed to be four, causing an increase in mesh number for both the wave height direction and wavelength direction. Fig. 3 shows the computed motion amplitudes for different mesh sizes and time steps when the incident wavelength is 1.2 times of the ship length in head sea condition. In this wave condition, the RAOs of the heave and pitch motions are close to peak. For the finest parameter, the uncertainty range is plotted and most cases show oscillatory behavior. The motion responses are especially dependent on the selected mesh size rather than the time step. The experimental value of the pitch motion is within the uncertainty band of the calculation results, while for the heave motion, the experiment result is out of the range of numerical uncertainty.

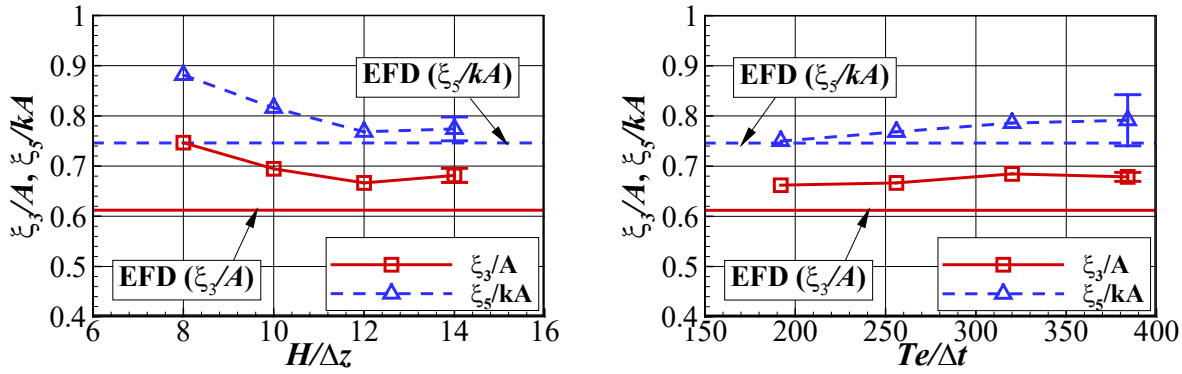

(a) Mesh (b) Time step

Figure 3: Uncertainty analysis for tumblehome in head waves (λ/L = 1.2, H/λ = 1/60, Fr = 0.2)

It can be easily understood that, from Fig. 3, the spatial discretization can be the main source of different solutions. However, the temporal discretization can also be the discrepancy source of the detailed flow. In Fig. 4, a snapshot of wave elevation distribution at the hull surface is plotted for different input time steps. Although the motion amplitudes seem not much sensitive to the time step, the detailed flow and free surface profile can be different for different time discretization. It can be seen that for the case of $Te/\Delta t$ = 192 shows some discrepancy from the other cases both in the bow and stern elevation. For the stern part of the ship, the elevation tends to converge when $Te/\Delta t$ is larger than the 320.

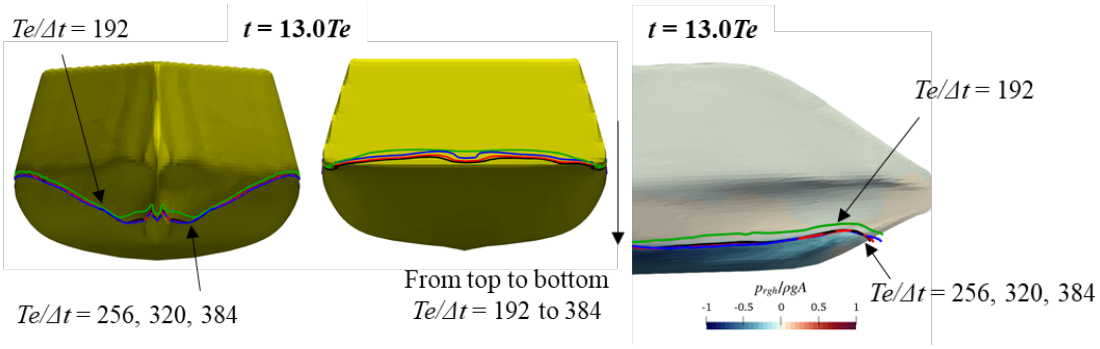

(a) Bow and stern view (b) Side view

Figure 4: Snapshot of wave elevation for depending on time step (λ/L = 1.2, H/λ = 1/60, Fr = 0.2)

4 CONCLUSIONS

In this study, the numerical uncertainty analysis is carried out for calm-water resistance computation and motion simulation in head waves. It is found that, for different ship speed, different mesh resolution is required to reduce the uncertainty level of steady wave resistance. For the ship motion in waves, it is harder to get the monotonic convergence for both the heave and pitch motions. For the present case, the dependency on the mesh is larger than that of the time step.

ACKNOWLEDGEMENT

This study was supported by the Lloyd's Register Foundation (LRF)-Funded Research Center at Seoul National University. Their support is greatly appreciated.

REFERENCES

[1] ITTC. 2017. *Recommended Procedure and Guidelines – Uncertainty Analysis in CFD Verification and Validation Methodology and Procedures*. Report 7.5-03-01-01.

[2] Roache, P. J. 1998. *Verification and Validation in Computational Science and Engineering*. (Hermosa publishers).

[3] Stern, F., Wilson, R. V., Coleman, H., Paterson, E. 2001. Comprehensive Approach to Verification and Validation of CFD-Simulations-Part 1:Methodology and Procedures. Journal of Fluid Engineering, 123(4), 793-802.

[4] Ellis, B. T. 1997. *An investigation into the damaged stability of a tumblehome hull warship design*. Master Thesis, Naval Postgraduate School.

[5] Kim, B.S., Park, D.M., Kim, Y. 2022. *Study on Nonlinear Heave and Pitch Motions of Conventional and Tumblehome Hulls in Head Seas*, Ocean Engineering, 247.